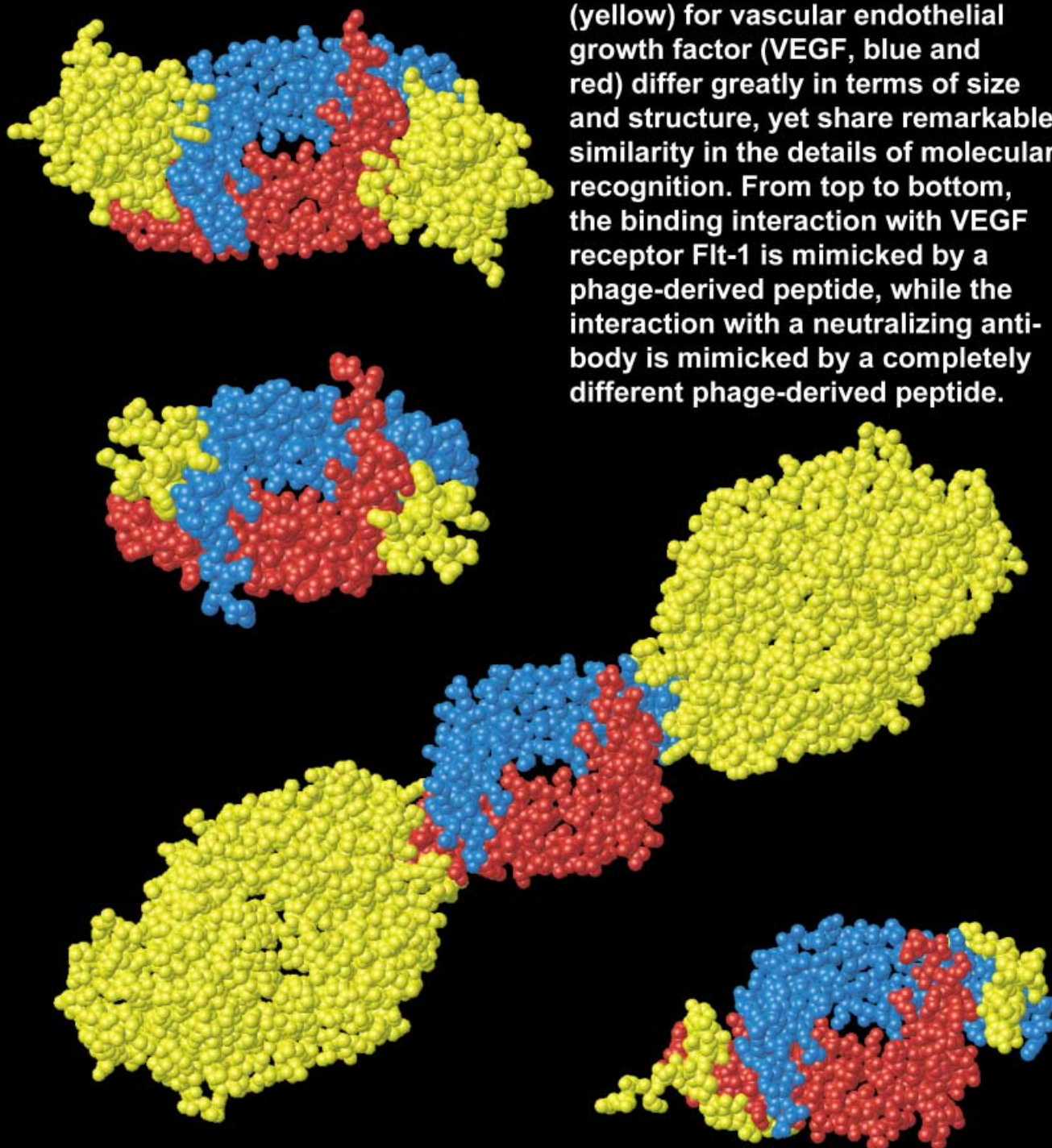


## Natural and nonnatural protein–protein interactions

Natural and nonnatural ligands (yellow) for vascular endothelial growth factor (VEGF, blue and red) differ greatly in terms of size and structure, yet share remarkable similarity in the details of molecular recognition. From top to bottom, the binding interaction with VEGF receptor Flt-1 is mimicked by a phage-derived peptide, while the interaction with a neutralizing antibody is mimicked by a completely different phage-derived peptide.



# Exploring Protein–Protein Interactions with Phage Display

Sachdev S. Sidhu,\* Wayne J. Fairbrother, and Kurt Deshayes<sup>[a]</sup>

*Protein–protein interactions mediate essentially all biological processes. A detailed understanding of these interactions is thus a major goal of modern biological chemistry. In recent years, genome sequencing efforts have revealed tens of thousands of novel genes, but the benefits of genome sequences will only be realized if these data can be translated to the level of protein function. While genome databases offer tremendous opportunities to expand our knowledge of protein–protein interactions, they also present formidable challenges to traditional protein chemistry methods. Indeed, it has become apparent that efficient analysis of proteins on a proteome-wide scale will require the use of rapid combinatorial approaches. In this regard, phage display is an established combinatorial technology that is likely to play an even greater role in the future of biology. This article reviews recent applications of phage display to the analysis of protein–protein interactions. With combinatorial mutagenesis strategies, it is now*

*possible to rapidly map the binding energetics at protein–protein interfaces through statistical analysis of phage-displayed protein libraries. In addition, naïve phage-displayed peptide libraries can be used to obtain small peptide ligands to essentially any protein of interest, and in many cases, these binding peptides act as antagonists or even agonists of natural protein functions. These methods are accelerating the pace of research by enabling the study of complex protein–protein interactions with simple molecular biology methods. With further optimization and automation, it may soon be possible to study hundreds of different proteins in parallel with efforts comparable to those currently expended on the analysis of individual proteins.*

## KEYWORDS:

combinatorial chemistry · phage display · protein engineering · protein–protein interactions

## 1. Introduction

Essentially all cellular processes depend on protein–protein interactions, and much of modern life-science research is concerned with first identifying natural interactions and second mapping the energetics and specificities of these interactions in fine detail. Such detailed knowledge can aid in determining the biological functions of novel proteins and also in the development of antagonists or agonists that can be used to further explore biology or even for therapeutic intervention. In the past few years, whole-genome sequencing projects have vastly expanded the database of novel genes, and we are now faced with tens of thousands of proteins with unknown functions.<sup>[1]</sup> The full benefit of genome sequences will only be realized if the information can be translated to the level of protein function, and to do this effectively and rapidly, researchers will need to adopt combinatorial biology approaches that can deal with large populations of proteins en masse.<sup>[2]</sup>

Phage display is one of the oldest and most powerful combinatorial biology methods (Figure 1). The technology is based on the fact that polypeptides fused to bacteriophage coat proteins can be displayed on phage particles that also contain the encoding gene.<sup>[3]</sup> In this way, a physical linkage between genotype and phenotype is established, and extremely diverse libraries ( $> 10^{11}$ ) of DNA-encoded peptides or proteins can be generated with simple molecular biology methods.<sup>[4]</sup> Furthermore, phage-displayed libraries can be amplified by passage through a bacterial host, and even the largest repertoires can be contained in less than one millilitre of solution. By using

selections with immobilized ligands, library pools can be enriched for polypeptides with particular binding traits. Following binding selection, individual clones from enriched pools can be analyzed by using simple enzyme-linked immunosorbent assays (ELISAs) to quantify binding in a high-throughput fashion.<sup>[4]</sup> Finally, and most importantly, the amino acid sequence of any clone can be readily deciphered by sequencing the DNA inside the phage particles.

Phage display has proven to be a robust technology that has had major impacts on numerous areas of biological chemistry.<sup>[5]</sup> In this review, we focus on applications in which the technology has been used to study protein–protein interactions, with recent examples from our own research. In particular, we highlight the application of combinatorial biology to three major areas of biochemical research: the mapping of binding energetics at protein–protein interfaces, the development of small synthesizable ligands to biologically active sites on proteins, and the characterization of natural protein–protein interactions in signaling pathways.

[a] Dr. S. S. Sidhu, Dr. W. J. Fairbrother, Dr. K. Deshayes  
Department of Protein Engineering  
Genentech, Inc.  
1 DNA Way  
South San Francisco, CA 94080 (USA)  
Fax: (+1) 650-225-3734  
E-mail: sidhu@gene.com

## 2. Mapping Functional Binding Epitopes within Protein–Protein Interfaces

Protein–protein interactions often involve numerous side chains from each protein; this results in the burial of large ( $>1000 \text{ \AA}^2$ ) surface areas at the contact interface.<sup>[6]</sup> Three-dimensional structures, obtained with either NMR spectroscopy or X-ray crystallography methods, have provided considerable insights into the mechanisms whereby proteins bind their partners with high affinity and specificity. However, while these

studies reveal structural epitopes, those residues that make intermolecular contacts at interfaces, they cannot define functional epitopes, the contact residues that also contribute energetically to the binding interaction. Accurate elucidation of functional epitopes requires mutagenesis strategies that can selectively alter particular side chains and binding assays that measure the effects of these mutations on protein function.<sup>[7]</sup> By combining structural and functional data, one can obtain three-dimensional views of the functional epitopes that mediate the binding energetics at protein–protein interfaces. These functional maps enhance our fundamental understanding of molecular recognition, and in practical terms, they provide valuable insights for rational protein and drug design.

Alanine scanning has proven to be a particularly powerful method for mapping functional binding epitopes.<sup>[7]</sup> In this method, individual protein residues are mutated to Ala, a substitution that removes atoms beyond the  $\beta$ -carbon atom and thus can be used to infer the roles of individual side chains.<sup>[8]</sup> Comparing the binding affinity of each Ala mutant to that of the wild type (wt) allows the effect of each side-chain truncation on the free energy of binding to be calculated from the equation  $\Delta\Delta G_{\text{Ala-wt}} = RT \ln(K_{a,\text{wt}}/K_{a,\text{Ala}})$ . This method was exemplified in pioneering studies of the high-affinity interaction between human growth hormone (hGH) site-1 and the hGH receptor (hGHbp).<sup>[7, 9, 10]</sup> The hGH–hGHbp binding interface involves more than 30 contact side chains from each protein. Each of these side chains was individually mutated to Ala, the mutant proteins were purified, and the affinities were determined with radioimmunoassays or surface plasmon resonance methods. Only a small subset of the contact side chains within each protein were found to contribute significantly to binding affinity, and when mapped onto the hGH–hGHbp complex structure, these side chains clustered into small and complementary functional epitopes or “hotspots”.<sup>[9]</sup> These studies demonstrated that, even within large structural epitopes, much of the binding energy responsible for molecular recognition may be supplied by significantly smaller functional epitopes, a fact suggesting that it may be possible to effectively mimic these interfaces with small inhibitors (see below).

Alanine scanning and other site-directed mutagenesis strategies have proven invaluable for the study of protein structure and function. However, these methods are not well suited for high-throughput protein analysis, because many individual mutants must be constructed, purified, and analyzed separately with protein chemistry methods that often require great skill and expertise. Recently, a combinatorial mutagenesis strategy, termed “shotgun scanning”, has been developed to expedite the exploration of protein structure and function.<sup>[11]</sup> This method uses phage-displayed protein libraries in which multiple sites are simultaneously mutated by using degenerate codons with restricted diversity. For example, in a shotgun alanine scan, codons are chosen to preferentially allow only the wt or Ala at each scanned position. Binding selections are then used to enrich for library members that retain affinity for a binding partner, and DNA sequencing of hundreds of binding clones is used to accurately determine the ratio of wt/mutant at each varied position within the selected pool. This ratio can be used to

*Sachdev Sidhu, born in 1968, studied chemistry at Simon Fraser University, where he investigated enzyme function under the supervision of Thor Borgord and obtained his PhD in 1996. Following a postdoctoral research fellowship with James Wells at Genentech, he joined the Protein Engineering Department there as a Scientist in 1998. His research interests focus on the use of combinatorial biology methods to explore protein structure and function.*



*Wayne Fairbrother, born in 1962, studied chemistry at the universities of Otago and Oxford. At Oxford he studied phosphate interactions with proteins under the supervision of R. J. P. Williams, FRS, and obtained his DPhil in 1989. Following a postdoctoral research fellowship with Peter Wright at The Scripps Research Institute, he joined the Protein Engineering Department at Genentech, Inc., in 1992, where he is currently a Senior Scientist. His research interests include using NMR spectroscopy to study the structure and dynamics of proteins, and protein–ligand and protein–protein interactions.*



*Kurt Deshayes, born in 1961, studied chemistry at Carleton College and the University of Chicago. At Chicago he studied organic synthesis and chemical recognition under the supervision of Jeffrey Winkler and obtained his PhD in 1988. Following a postdoctoral research fellowship with Donald J. Cram at the University of California, Los Angeles, he joined the chemistry faculty at Bowling Green State University in 1990 and joined the Protein Engineering Department at Genentech, Inc., in 1998, where he is currently a Scientist. His research interests include chemical recognition and focus on protein–protein interactions.*



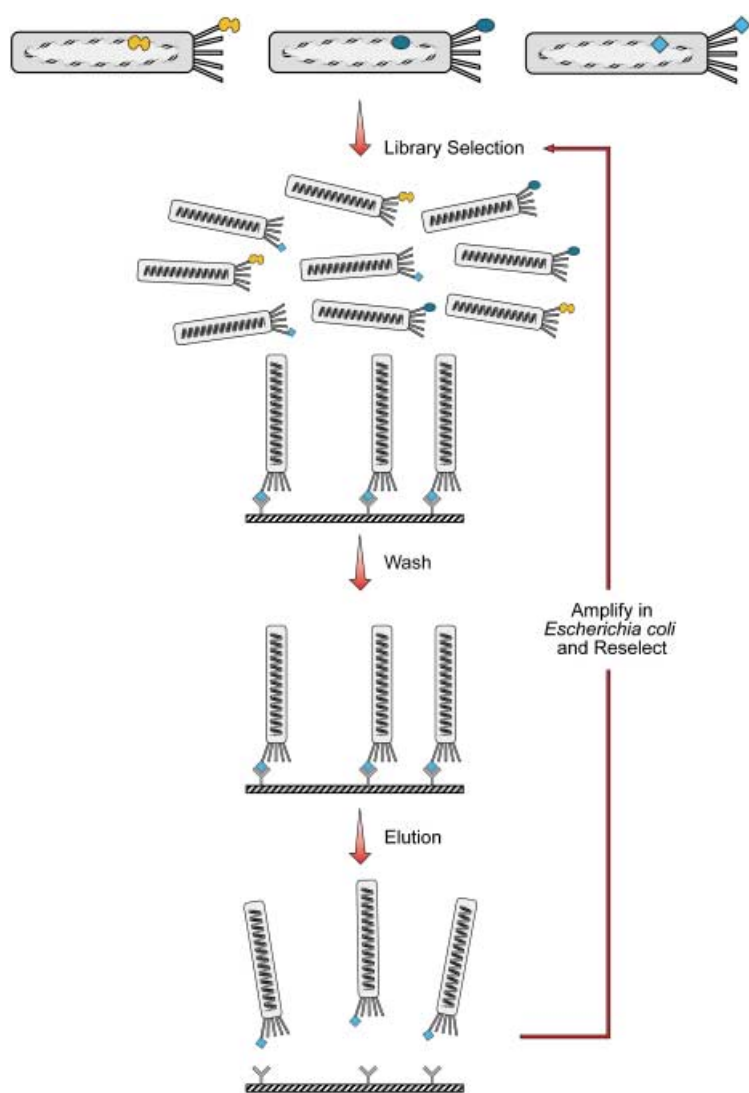


**Figure 1.** In vitro selection with phage display. Polypeptides are displayed on phage particles that also contain the encoding DNA. Display is usually achieved by fusion to either the gene-3 minor coat protein which is located at one end of the particle (shown) or the gene-8 major coat protein which covers the length of the particle. The library is incubated with an immobilized target to select for binders, and nonbinding phage are removed by washing. Bound phage are then eluted and amplified in *E. coli*. Amplified phage pools can be subjected to additional rounds of selection, or alternatively, the sequences of individual binding polypeptides can be determined by sequencing the encapsulated DNA.

quantitatively assess the effect of each mutation on the binding interaction. The method is rapid and amenable to high-throughput analysis because many side-chains are simultaneously scanned with a single library by using simple molecular-biology techniques that circumvent the need for protein purification and biophysical analysis.

Shotgun scanning was first used to reiterate the conventional hGH site-1 alanine scan described above, but in a combinatorial fashion.<sup>[11]</sup> Nineteen residues in the hGH site-1 structural epitope for binding to hGHbp were mutated in a single library that was cycled through two separate selections. The first selection was a “structural selection” for variants retaining affinity for a monoclonal antibody that required native hGH structure but bound to

hGH at a site distinct from the structural epitope for hGHbp. The second selection was for binding to hGHbp itself, and this “functional selection” required not only native hGH structure but also selected for residues within the structural epitope that made energetic contributions to the interaction with hGHbp. Several hundred binding clones from each selection were sequenced, and the wt/Ala ratios ( $n_{wt}/n_{Ala}$ ) were determined for each scanned position (Figure 2A).

Since the wt/Ala ratio correlates with a side chain’s contribution to the selected trait (that is, structure and/or function), statistical “ $\Delta\Delta G^{stat}$ ” values were determined for the effect of each side-chain mutation on each selection by using the equation  $\Delta\Delta G^{stat} = RT \ln(n_{wt}/n_{Ala})$ , in analogy with the standard equation for point mutations ( $\Delta\Delta G_{Ala-wt} = RT \ln(K_{a,wt}/K_{a,Ala})$ ). Finally, for each mutation, the  $\Delta\Delta G^{stat}$  value for the structural selection was subtracted from the  $\Delta\Delta G^{stat}$  value for the functional selection; this process was to correct for structural effects and left a corrected  $\Delta\Delta G_{Ala-wt}$  value that presumably measured the contribution of each side chain to the functional epitope. These statistical  $\Delta\Delta G_{Ala-wt}$  values were found to be in good agreement with  $\Delta\Delta G_{Ala-wt}$  values determined with conventional alanine scanning, a fact demonstrating the validity of the statistical approach (Figure 2B). Both conventional and shotgun alanine scanning reveal that only a small subset of contact side chains contribute significantly to the binding interaction with hGHbp, and these form a compact functional epitope in the hGH tertiary structure (Figure 2C).

Shotgun scanning mutagenesis is a general strategy that can be applied to any protein that can be displayed on phage. Recently, the method has been used to investigate the antigen-binding site of Fab2C4, the antigen-binding fragment of an antibody that binds to the human oncogene product ErbB2.<sup>[12]</sup> In this study, an alanine scan was performed with 4 libraries that together covered 61 out of 64 side chains in the complementarity determining regions (CDRs). This comprehensive analysis investigated not only the solvent-exposed residues that can potentially make direct contact with the antigen, but also buried scaffolding residues that hold these contact residues in a binding-competent conformation. Furthermore, the rapidity of shotgun scanning allowed for a separate homologue scan that tested the effects of subtle, chemically similar substitutions (Phe for Tyr, Glu for Asp, etc.). When mapped onto the Fab2C4 crystal structure, these data provided distinct, yet complementary, functional views of the antigen-binding site. Interestingly, the alanine scan revealed a 610 Å<sup>2</sup> functional epitope surface that shrank to only 369 Å<sup>2</sup> when mapped with homologous substitutions; this suggests that this smaller subset of side chains common to both scans may be involved in precise contacts with the antigen.

Since shotgun scanning relies on statistical analysis of combinatorial libraries, there will be uncertainty associated with



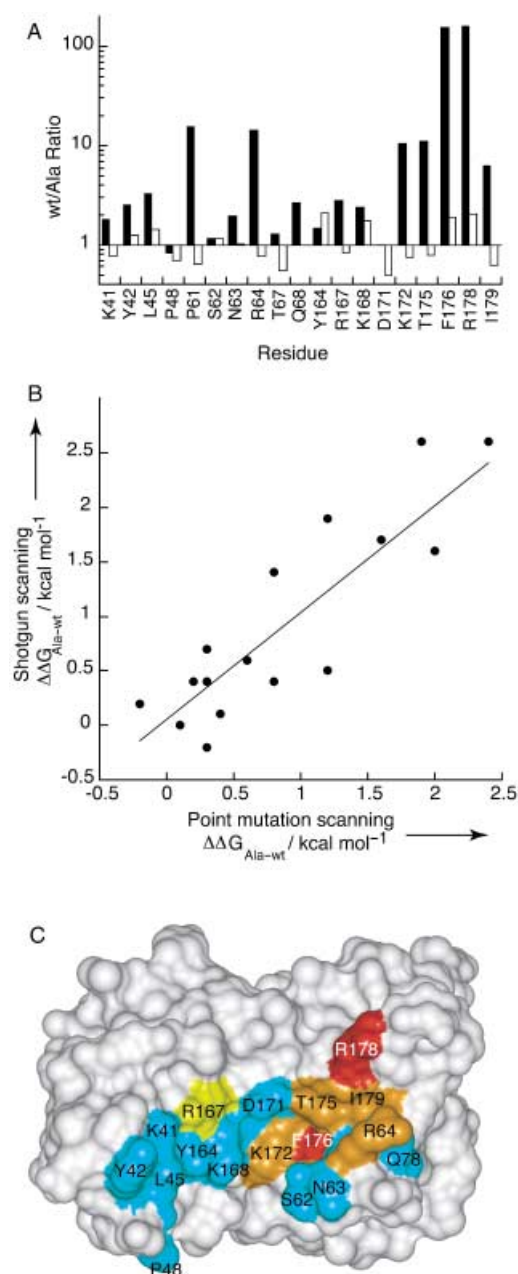


**Figure 2.** Shotgun alanine scan of hGH. A) Following either a “structural” or “functional” selection (white or black bars, respectively), the wt/Ala ratios at 19 mutated positions were determined by sequencing several hundred binding clones. Ratios greater than or less than one indicate mutations that are deleterious or beneficial to the selected trait, respectively. The wt/Ala ratios can be used to calculate the change in the free energy of binding for each Ala mutant relative to wt ( $\Delta\Delta G_{Ala-wt}$ ). B)  $\Delta\Delta G_{Ala-wt}$  values determined by shotgun scanning (y axis) are in good agreement with those determined by conventional alanine scanning (x axis) that involved the analysis of purified point-mutated proteins with surface plasmon resonance spectroscopy. The least squares linear fit of the data is shown ( $y = -0.01 + 1.0x$ ;  $R = 0.88$ ). C) When mapped onto the structure of hGH (PDB accession code 3HHR),<sup>[58]</sup> the shotgun-scan results reveal a compact functional epitope composed of a small subset of contact side chains that contribute most of the binding energy to the interaction with hGHbp. Residues are colored according to their statistical  $\Delta\Delta G_{Ala-wt}$  values obtained from the shotgun alanine scan: red,  $\Delta\Delta G_{Ala-wt} > 2.0 \text{ kcal mol}^{-1}$ ; orange,  $1.3 < \Delta\Delta G_{Ala-wt} < 2.0 \text{ kcal mol}^{-1}$ ; yellow,  $0.6 < \Delta\Delta G_{Ala-wt} < 1.3 \text{ kcal mol}^{-1}$ ; cyan,  $\Delta\Delta G_{Ala-wt} < 0.6 \text{ kcal mol}^{-1}$ . The shotgun-scanning data were taken from ref. [11] by Weiss et al., while the conventional alanine-scan data were from ref. [10] by Cunningham and Wells. See the main text for further details.

predictions relating to the effects of any individual mutation. Thus, combinatorial methods of protein analysis are best viewed as a complement to detailed biophysical analysis. Shotgun scanning can be used to rapidly gather information across a protein–protein interface, and the data obtained can be used to generate hypotheses that can then be tested in detail by quantitative analysis of point-mutated proteins. By combining the different approaches, it should be possible to gain a better understanding of protein–protein interactions than would be possible with either method alone.

### 3. Peptidic Mimics of Extracellular Protein Binding Surfaces

As discussed above, mutagenesis and structural studies have revealed that, while extracellular protein–protein interactions usually involve contacts over large surface areas, these interfaces often contain smaller functional epitopes where a substantial proportion of the binding energy is concentrated. In this section, we discuss applications of “naïve” (that is, completely random) peptide libraries in exploring these surfaces.

Peptides can be displayed on M13 phage in either a high- or low-valency format by fusing to either the gene-8 major coat protein (protein-8, P8) or the gene-3 minor coat protein (protein-3, P3), respectively.<sup>[4]</sup> The avidity inherent in polyvalent display magnifies intrinsic monovalent affinity so that even moderate-affinity peptides with dissociation constants in the high micromolar range are tightly bound to the target. In contrast, avidity effects are eliminated or greatly reduced in a low-valency format, thus allowing for discrimination and selection on the basis of even slight differences in intrinsic affinity. The complementary properties of high- and low-valency display have been used to develop a general process for selecting binding peptides from phage-displayed libraries, as outlined in Figure 3.

Initially, naïve peptide libraries are displayed in a polyvalent format on P8, and the use of libraries with greater than  $10^{11}$  individual members allows for rapid sampling of significant sequence space. Polyvalent library pools are cycled through rounds of binding selections to isolate peptides that bind specifically to the target, and high-throughput phage ELISAs are used to monitor the selection process and to identify individual binding clones. If the selection process is continued for only a minimal number of rounds, binders will be enriched without stringently discriminating between individual binding clones. Under these conditions, large naïve libraries can yield multiple, unique binders that can be grouped into families on the basis of sequence similarity.<sup>[13]</sup> This process identifies dominant scaffolds that may be well suited for binding to a particular target, and these can be used to design focused second generation libraries for affinity optimization.

Second generation libraries are usually displayed in a low-valency format on P3 to enable stringent selection and evolution of high-affinity binders through a combination of changes in peptide structure and/or interacting side chains.<sup>[4, 13]</sup> Furthermore, the affinities of low-valency, phage-borne peptides are

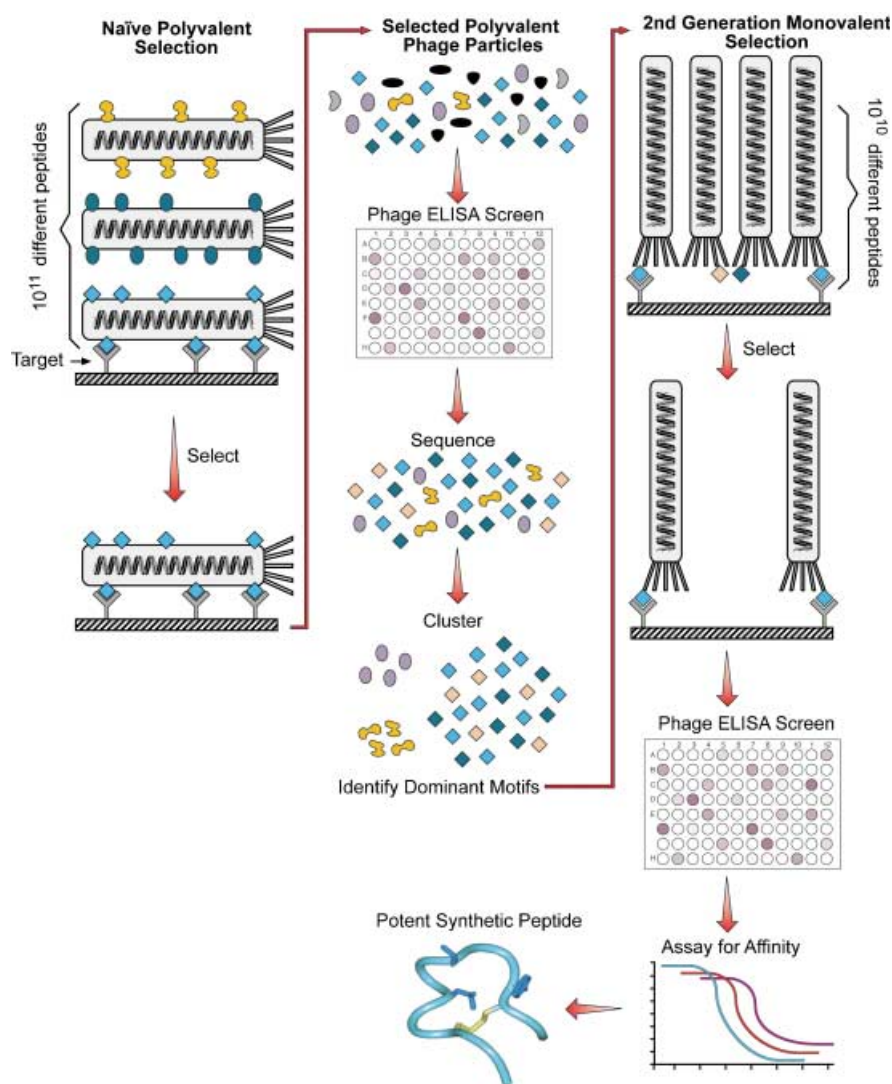


**Figure 3.** The process for selection and affinity maturation of binding peptides from phage-displayed libraries. Naïve peptide libraries are usually displayed in a high-valency format by fusion to the gene-8 major coat protein, thus enabling polyvalent binding interactions that magnify the apparent affinities of initial weak binders. High-throughput phage ELISAs in a 96-well format can be used to screen hundreds or even thousands of clones to identify genuine binders for sequence analysis, and the sequences of many unique binders can be used to identify dominant motifs that share sequence homology. This information can be used to design tailored second-generation libraries for affinity maturation in a low-valency format by fusion to the gene-3 minor coat protein. Stringent selections enable discrimination on the basis of intrinsic monovalent affinity, and the affinities of phage-borne peptides can be accurately determined with modified phage ELISAs. In the end, this ensures that synthetic peptides designed on the basis of phage data are likely to be potent binders.

usually in good agreement with the intrinsic affinities of free peptides; this allows continuous monitoring of the selection process with rapid phage ELISAs.<sup>[4, 13]</sup> Once the selection process has identified potent sequences, peptides are synthesized and subjected to detailed analysis of structure and function. When combined with high-throughput sequencing and assays, the phage-displayed peptide libraries may be used to simultaneously evolve several distinct families of binding peptides that could potentially lead to the discovery of multiple ligands for a single target protein. A collection of unique phage-derived peptides that bind to a single target can be expected to provide useful probes of the binding surface.

As extracellular protein–protein interactions typically involve large surfaces void of significant concavity, conventional small-molecule screening efforts have generally failed to identify antagonists for these interactions.<sup>[14]</sup> In contrast, phage-displayed peptide libraries have proven remarkably successful in generating both antagonists and agonists for numerous extracellular targets.<sup>[13, 15–24]</sup> Since phage do not operate under the same pressures that influenced the evolution of natural binding partners, it is reasonable to believe that epitopes distinct from those found on the natural ligands will be discovered. A related seductive notion is that phage display will identify localized binding epitopes that might be readily transferred to potent small-molecule scaffolds.

The success of phage display in identifying ligands to protein surfaces allows us to address important questions. For example, what types of interactions are found for phage-derived binding peptides, and how do the peptide-binding surfaces compare to the naturally evolved binding surfaces of large protein ligands? Furthermore, are the peptide interactions likely to be mimicked by small organic molecules? Substantial insights into molecular recognition have been afforded by structural studies of peptides that bind protein surfaces, and several of these structures are shown in Figure 4.

Peptides containing at least one internal disulfide bond have been selected consistently against extracellular targets. The constraints imposed by disulfide bonds can stabilize peptide solution structures and thus yield preorganized binding surfaces. Although structure is uncommon for peptides in general, the observation that selection for binding to extracellular proteins frequently yields

structured peptides is noteworthy<sup>[13, 17, 20, 23, 24]</sup> and suggests that preorganized structure may be a prerequisite for high-affinity binding to such surfaces. Peptides that bind to a variety of targets have often been found to have  $\beta$  hairpin or turn–helix structures, but other unusual folds have also been observed (Figure 4).<sup>[13, 15–17, 19–25]</sup> While a comprehensive review of the peptide–phage literature is beyond the scope of this article, the major points raised by these studies can be addressed by examining the substantial structural database of complexes between vascular endothelial growth factor (VEGF) and various ligands. Specifically, we will compare the interactions between VEGF and two different phage-derived peptides to those that

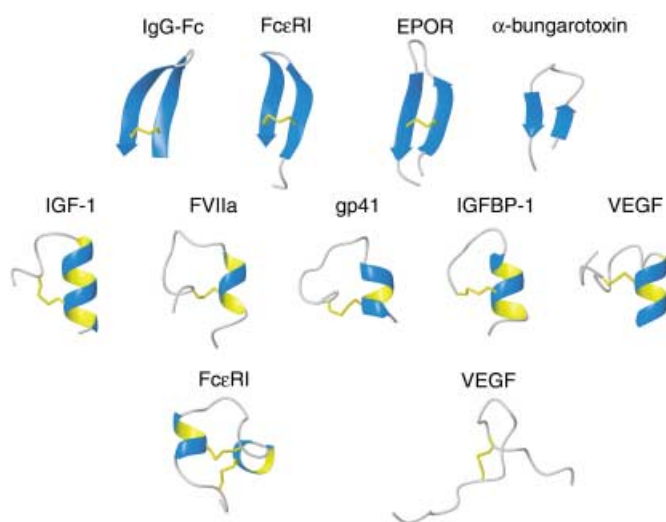


**Figure 4.** Phage-derived peptide antagonists and agonists for which structures have been determined free in solution and/or bound to their target proteins. Elements of secondary structure are shown as ribbons and disulfide-bonded cysteine side chains are shown in yellow. The target proteins are indicated above the peptide structures in each case. The PDB accession codes for each peptide are as follows: IgG-Fc, 1DN2;<sup>[21]</sup> FcεRI (hairpin peptide), 1JBF;<sup>[23]</sup> EPOR, 1EBP;<sup>[15]</sup> α-bungarotoxin, 1HAA;<sup>[22]</sup> IGF-1, 1LB7;<sup>[13]</sup> FVIIa, 1DVA;<sup>[20]</sup> gp41, 1CZQ;<sup>[19]</sup> IGFBP-1, 1GJE;<sup>[36]</sup> VEGF (v107), 1KAT;<sup>[25]</sup> FcεRI ("zeta" peptide), 1KCO;<sup>[24]</sup> VEGF (v108), 1VPP.<sup>[34]</sup> This figure was produced with the program MOLMOL.<sup>[59]</sup>

VEGF makes with one of its receptors or with neutralizing antibodies.

VEGF is a primary modulator of physiological angiogenesis that is also associated with pathological states such as cancer, rheumatoid arthritis, and psoriasis.<sup>[26]</sup> VEGF exists in solution as a homodimer and functions by binding to and inducing dimerization of its tyrosine kinase receptors, Flt-1 (*fms*-like tyrosine kinase-1; VEGFR-1) and KDR (kinase-insert domain containing receptor; VEGFR-2). Activation of KDR alone is sufficient to stimulate vascular endothelial cell mitogenesis.<sup>[27]</sup> Flt-1, on the other hand, may act as a "decoy" receptor that is able to negatively regulate angiogenesis by sequestering VEGF.<sup>[28]</sup> A high-resolution crystal structure of VEGF in complex with the second Ig-like domain (D2) of Flt-1 (Flt-1<sub>D2</sub>) revealed symmetrical receptor-binding sites located at the poles of the dimeric VEGF receptor-binding domain,<sup>[29]</sup> and alanine-scanning mutagenesis revealed very similar KDR-binding sites.<sup>[30, 31]</sup> The binding sites for several antibodies that bind and neutralize VEGF have also been shown to overlap with the KDR- and Flt-1-binding sites.<sup>[31–33]</sup>

In order to discover novel antagonistic molecules, a library of disulfide-constrained peptides was sorted against VEGF. Three distinct peptide classes were isolated and affinity matured, and it was shown that each class not only binds to VEGF but also blocks its interactions with KDR.<sup>[18]</sup> Representatives of two of these peptide classes, v108 (class 2; RGWVEICAADDYGRCLTEAQ) and

v107 (class 3; GGNECDIARMWEWECFERL), have subsequently had their structures determined in complex with the VEGF receptor-binding domain (Figure 5 A and B).<sup>[25, 34]</sup>

The structures reveal that the binding sites for both peptides overlap significantly with the receptor and antibody binding sites and with each other; this latter fact is consistent with the observation that v108 competes with v107 for binding to VEGF.<sup>[18]</sup> The contact between v108 and VEGF involves primarily main-chain-mediated hydrogen bonds, while in contrast, v107 makes extensive hydrophobic side-chain-mediated contacts with VEGF. Neither binding mode is unique, however, since each peptide complex resembles another structurally characterized VEGF complex. The v107 interaction with VEGF is most similar to that observed for Flt-1<sub>D2</sub>,<sup>[29]</sup> while the binding mode of v108 most closely resembles that of an antigen-binding fragment (Fab) from a neutralizing anti-VEGF antibody (Figure 5 C and D).<sup>[32, 33]</sup> A survey of the literature shows that these results are not uncommon, in that most binding sites for phage-derived peptides overlap with and block binding sites for natural ligands (see Figure 4). This suggests that protein-binding sites may have physical properties that predispose them to ligand binding.<sup>[21, 35]</sup>

Although the modes of interaction are similar, the dissociation constant ( $K_d$ ) values of the phage-derived peptides (0.6 or 2.2  $\mu\text{M}$  for v107 or v108, respectively)<sup>[18, 25]</sup> are significantly weaker than the 2–10 nM reported for Flt-1<sub>D2</sub> and 13 nM or 0.11 nM reported for a humanized anti-VEGF Fab (Fab-12) or its affinity-optimized version (Fab-Y0317), respectively.<sup>[25, 29, 33]</sup> Nevertheless, it is impressive that phage display can identify a 19-residue peptide, v107, that buries 1167 Å<sup>2</sup> of hydrophobic binding surface. The structure of the v107–VEGF complex further reveals that the four N-terminal residues of the peptide are disordered and do not contact the protein, which suggests that a 15-residue peptide would be sufficient for binding. In contrast to the v107

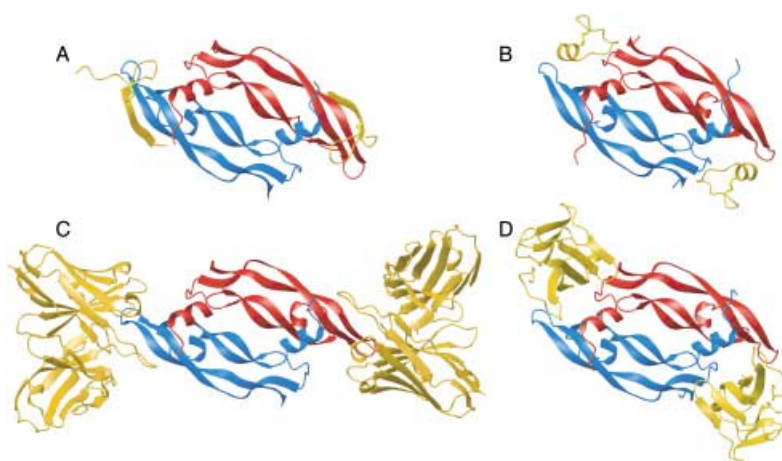


**Figure 5.** Structures of the VEGF receptor-binding domain in complex with peptide and protein ligands. A) Crystal structure of the VEGF–v108 complex (PDB accession code 1VPP). B) Solution structure of the VEGF–v107 complex (PDB accession code 1KAT). C) Crystal structure of VEGF in complex with the Fab fragment of a neutralizing antibody (PDB accession code 1CZ8). Only the Fv region of the Fab is shown. D) Crystal structure of the VEGF–Flt-1<sub>D2</sub> complex (PDB accession code 1FLT). In each case the VEGF monomers are colored red and blue, respectively, and the bound ligands are colored yellow. This figure was produced with the program MOLMOL.<sup>[59]</sup>



complex, Flt-1<sub>D2</sub> uses 101 residues to bury a total surface area of 1672 Å<sup>2</sup>. Notably, all the VEGF residues that contact v107 in the peptide complex also contact Flt-1 in the receptor complex. Equally remarkable is the fact that a 20-residue peptide, v108, buries a total surface area of 1350 Å<sup>2</sup> on binding VEGF, while the receptor-blocking Fabs bury 1750–1800 Å<sup>2</sup>. In this case, the seven C-terminal residues of the peptide have no contacts with VEGF. Of these seven residues, Cys15 is clearly required to maintain the bound structure of the peptide in the complex, but truncation of the four C-terminal residues has only a minimal effect on VEGF binding affinity.<sup>[18, 34]</sup> While only 5 of the 13 VEGF residues in the interface with v108 make contacts with Flt-1<sub>D2</sub>, 12 of these 13 residues are also involved in contacts in the VEGF–Fab complexes. As noted above, the v107 and receptor interfaces are dominated by hydrophobic interactions. In contrast, up to 13 intermolecular hydrogen bonds are observed in the interface of the v108 complex while 10–12 are found in the Fab complexes. (Note that v108 does not bind in a unique conformation and that two slightly different sets of peptide–protein interactions are observed in the crystal structure of the complex.) Most notably, all VEGF atoms involved in conserved hydrogen bonds in the v108 complex also form hydrogen bonds to the Fabs.

Functional characterization of the VEGF–v107 interface was achieved by alanine scanning both the peptide and VEGF contact surfaces.<sup>[25]</sup> Comparison of the functional epitopes on VEGF for binding to v107 or Flt-1<sub>D2</sub> revealed some distinct differences but also showed that peptide and receptor binding require similar numbers of functionally important residues. Interestingly, in each case, alanine substitution of six VEGF residues resulted in >10-fold reductions in binding affinity; important v107 binding determinants include Tyr21, Tyr25, Lys48, Leu66, Met81, and Met83, while the most important Flt-1<sub>D2</sub>-binding determinants are Phe17, Met18, Tyr21, Gln22, Tyr25, and Leu66 (Figure 6B and C). Apparently, although the VEGF structural epitope for v107 binding is ≈30% reduced relative to that for Flt-1<sub>D2</sub> binding, the VEGF functional epitope for peptide binding is no more localized than that for receptor binding, which suggests that transfer of this novel peptide epitope to a potent small-molecule scaffold may be difficult.

Compounding this difficulty is the observation that the energetic contributions of the hydrophobic side chains of v107 to VEGF binding are not additive.<sup>[25]</sup> A complete alanine scan of the hydrophobic residues that constitute the structural binding epitope of v107 revealed that the sum of the individual side-chain contributions ( $\Delta\Delta G \geq 18$  kcal mol<sup>-1</sup>) is significantly greater than the total binding energy ( $\Delta G \approx -8$  kcal mol<sup>-1</sup>), which suggests that cooperativity exists between peptide structural stabilization and binding. In particular, the side chains of Trp11 and Phe16 have significant intramolecular contacts with each other and with the surrounding hydrophobic side chains (Ile7, Met10, Trp13, and Leu19; Figure 6A). Substitution of either of these side chains with the methyl group of alanine results in >2000-fold reductions in binding affinity for VEGF; a substantial fraction of this loss probably results from destabilization of the bound peptide conformation. Unfortunately, in this case, there is no way to check the structural consequences of the alanine

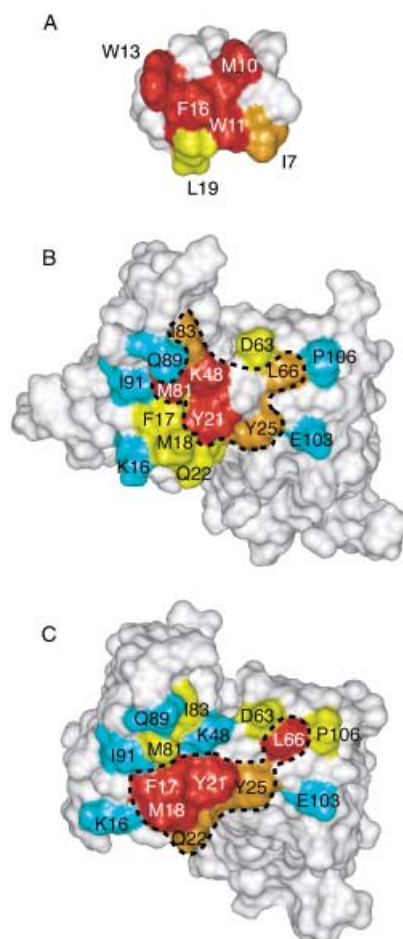


**Figure 6.** Comparison of alanine-scanning data for A) v107 binding to VEGF, B) VEGF binding to v107, and C) VEGF binding to Flt-1<sub>D2</sub>. Residues are colored according to the relative  $IC_{50}$  values of their respective alanine mutants as follows: red, > 30-fold increase ( $\Delta\Delta G_{Ala-wt} > 2.0$  kcal mol<sup>-1</sup>); orange, 10–30-fold increase ( $1.3 < \Delta\Delta G_{Ala-wt} < 2.0$  kcal mol<sup>-1</sup>); yellow, 3–10-fold increase ( $0.6 < \Delta\Delta G_{Ala-wt} < 1.3$  kcal mol<sup>-1</sup>); cyan, < 3-fold increase ( $\Delta\Delta G_{Ala-wt} < 0.6$  kcal mol<sup>-1</sup>).

substitutions on the free peptide because v107 does not have a well-definable structure in the absence of VEGF.

Results similar to those for the VEGF–v107 interface have been observed in other systems. For instance, the functional binding epitope for the phage-derived peptide E-76 on coagulation factor VIIa (FVIIa) is also not well localized.<sup>[20]</sup> In addition, peptide alanine-scanning data show that the sum effect of substituting interface residues (as identified from a crystal structure of the FVIIa–E-76 complex) with alanine is significantly greater than the total binding energy.<sup>[20]</sup> In this case, NMR spectroscopy structural data confirmed that some of the peptide mutants are structurally perturbed relative to E-76. Such non-additivity in the effects of alanine substitutions seems to be common amongst phage-derived peptides (at least in the limited number of cases in which alanine-scanning data are reported)<sup>[20, 23, 24, 36]</sup> and it is most likely the “price that must be paid” for minimizing a protein scaffold to a peptide scaffold (that is, important protein-binding determinants on the peptide are frequently also important for maintaining peptide structure). In particular, members of the turn–helix structural class of



peptides,<sup>[13, 19, 20, 25, 36]</sup> which includes v107, each have a cluster of hydrophobic residues on one face that has been shown to be important for peptide structural stability<sup>[20, 36]</sup> and for direct contact with respective target proteins.<sup>[19, 20, 25]</sup>

The fact that phage-derived peptides adopt VEGF-binding interactions similar to those observed for natural protein ligands is probably not due to random chance; rather, it suggests that only limited regions of the VEGF surface can support high-affinity binding interactions. The phage-derived peptides are significantly smaller than either antibodies or proteins, but they still bind to the same epitopes. An illuminating comparison can be made between the interfaces described above and data obtained from crystal structure analysis of protein–protein complexes. Examination of 32 protein dimer structures revealed that the size of the protein–protein interfaces ranged from 368 to 4761 Å<sup>2</sup>,<sup>[37]</sup> while a similar analysis of protease inhibitor complexes and antibody–protein–antigen complexes showed a range of 1600 ± 350 Å<sup>2</sup>.<sup>[38]</sup> Thus, VEGF-binding peptides present interaction surfaces on reduced scaffolds, but the buried surface areas in these peptide–protein interfaces (≈ 1000 Å<sup>2</sup>) fall within the observed norms for protein–protein interactions; this suggests that it will be difficult to develop small molecules that bind to VEGF with high affinity.

The inability of phage display to identify small-molecule-binding sites on extracellular proteins is not due to a lack of epitopes being presented to the target protein. Increases in library diversity to greater than 10<sup>11</sup> individual members have not changed the types of peptides being discovered, so it appears that peptides that resemble “miniproteins” are probably the only tight binders to many extracellular proteins. As always, there are exceptions (for example, the integrins) in which extracellular proteins have evolved binding sites for small epitopes, but the majority of extracellular proteins studied to date have given results similar to the VEGF example. Thus we conclude that, if diverse peptide libraries only yield ligands that present binding surfaces characteristic of a larger protein, the protein is unlikely to be a good target for small-molecule ligands.

#### 4. Mapping Intracellular Protein–Protein Interactions

While most extracellular protein–protein interactions involve large epitopes formed by discontinuous regions of primary sequence, there are numerous intracellular interactions that depend on the specific recognition of small, continuous epitopes within large proteins. Indeed, many distinct families of intracellular protein domains have evolved to recognize linear epitopes with particular characteristics.<sup>[39]</sup> Proline-rich sequences are recognized by at least two different families: Src homology 3 (SH3) domains<sup>[40]</sup> and WW domains (named for two highly conserved tryptophan residues within the family consensus).<sup>[41]</sup> Another common binding motif consists of phosphotyrosine-containing sequences, which are recognized by Src homology 2 (SH2)<sup>[42]</sup> and phosphotyrosine-binding (PTB) domains.<sup>[43]</sup> PDZ domains (so-called because they were first recognized in the proteins postsynaptic density-95, discs large, and zonula occlu-

dens-1) predominantly bind to specific C-terminal sequences.<sup>[44]</sup> These and other peptide-binding domains are small compact modules that are usually found imbedded in larger proteins, often with other modules of their own or different types. Acting in concert, multiple modules can bind multiple partners and thus assemble and localize intricate signaling complexes and intracellular architecture.

Phage-displayed peptide libraries have proven to be ideal tools in analyzing these intracellular peptide-binding domains. In many cases, small unconstrained peptides (four to eight residues) have proven to be remarkably specific, high-affinity ligands. We discuss the use of phage display in exploring ligand specificity in several domain families where peptides have been used to understand the relationships between structure and function, and also to predict and validate natural protein–protein interactions.

Several studies have focused on identifying peptide ligands for SH3 domains.<sup>[45, 46]</sup> These analyses have usually yielded proline-rich sequences similar to those found in natural SH3 ligands, but notably, some phage-derived peptides were found to bind with higher affinity than natural ligands.<sup>[46]</sup> While early studies confirmed the SH3-binding specificities defined by other methods, more recent work has identified binding motifs that do not match the “classical” consensus sequences for SH3 ligands, thereby suggesting that SH3-binding specificities may be more diverse than originally thought.<sup>[47]</sup> Studies of WW domains have also been successful in identifying binding sequences that resemble natural proline-rich ligands.<sup>[48]</sup> In many of these studies, phage-derived sequences have been used to predict natural binding partners by database mining, and also to guide mutagenesis and structural studies that shed further light on the structural features that mediate affinity and specificity. In a recent report, the specificities of approximately 20 yeast SH3 domains were studied with both peptide–phage and yeast-two-hybrid methods, and the two data sets were used to generate independent protein interaction networks by database mining of the complete yeast genome.<sup>[49]</sup> By comparing the two maps to each other, it was possible to obtain a third interaction network that represents the intersection of the two data sets and, thus, is likely to contain a greater proportion of physiologically relevant interactions.

Reversible tyrosine phosphorylation and dephosphorylation regulates many intracellular signaling pathways by modulating enzyme activities and creating or eliminating protein–protein interactions. These effects are often mediated by protein domains that bind to particular phosphotyrosine-containing sequences.<sup>[39, 44]</sup> While it has been difficult to investigate these interactions with phage display due to the lack of protein phosphorylation in *E. coli*, it has been shown that phage-displayed peptide libraries can be phosphorylated *in vitro*. These phosphorylated libraries have been used to study the binding specificities of both SH2 and PTB domains.<sup>[50]</sup> In each case, tyrosine-containing consensus sequences were identified for the different domains. These results demonstrate that *in vitro* posttranslational modifications may prove useful in further extending the utility of phage display and other combinatorial methods.

PDZ domains occur in a large variety of eukaryotic proteins, and in general, they are responsible for assembling other proteins into functional complexes localized at specific subcellular sites, such as epithelial tight junctions or neuronal synaptic densities.<sup>[51]</sup> In an early work, we developed libraries of novel C-terminally phage-displayed peptides to investigate the binding specificities of two of the six PDZ domains from a membrane-associated guanylate kinase (MAGI-3).<sup>[52]</sup> Each domain bound specifically to small peptides and the binding specificities were very different from each other, which suggests that the two PDZ domains bind different ligands. Like many PDZ-containing proteins, MAGI-3 contains multiple PDZ domains, and thus, a single MAGI-3 protein probably acts as a multiligand scaffold to assemble multicomponent protein complexes.

More recently, we used C-terminal peptide–phage libraries to study the binding specificity of the single PDZ domain of Erbin,<sup>[53]</sup> a protein that was originally identified as a putative ligand for ErbB2 in a yeast-two-hybrid screen.<sup>[54]</sup> ErbB2 is a tyrosine kinase related to the epidermal growth factor receptor and is a causal factor in the development of some cancers,<sup>[55]</sup> and our original intent was to discover high-affinity ligands for the Erbin PDZ domain that could be used to disrupt its interaction with ErbB2. Surprisingly, phage display revealed a binding consensus for Erbin PDZ ([D/E][T/S]WV<sub>COOH</sub>) that differed significantly from the C-terminal sequence of ErbB2 (DVPV<sub>COOH</sub>). Furthermore, searches of genomic databases revealed that the phage-derived consensus closely matched the C termini of  $\delta$ -catenin and two related homologues (ARVCF and p0071), which all terminate in an identical sequence (DSWV<sub>COOH</sub>). Since these catenins are also mediators of intracellular signaling,<sup>[56]</sup> it seemed reasonable that they could interact with Erbin in a physiologically relevant manner. Subsequent *in vitro* and *in vivo* experiments clearly demonstrated that Erbin binds to  $\delta$ -catenin and its homologues with high affinity and specificity, while its affinity for ErbB2 is significantly lower. Furthermore, the *in vivo* interaction between Erbin and ARVCF was successfully disrupted by intracellular delivery of phage-derived high-affinity peptides, a fact suggesting possible utility for peptide ligands in intracellular target validation.<sup>[53]</sup>

In studying the relationships between PDZ domain structure and function, we have made extensive use of *in vitro* affinity assays with synthetic peptides to accurately map the determinants of affinity and specificity. Our results suggest that PDZ domains can use up to five side chains at the C termini of proteins to bind with high affinity to their cognate ligands while excluding other closely related sequences. This point was illustrated by comparing the binding specificity of the Erbin PDZ domain to that of MAGI-3 PDZ2. Peptide–phage libraries revealed that these two domains recognize C-terminal consensus sequences that differ at only one site in the last four positions ([D/E][T/S]WV<sub>COOH</sub> versus [C/V/I][T/S]WV<sub>COOH</sub> for Erbin PDZ or MAGI-3 PDZ2, respectively). However, this single difference was sufficient to alter affinity by at least two orders of magnitude; a peptide bearing a Glu side chain (TGWETWV<sub>COOH</sub>) interacted exclusively with the Erbin PDZ domain while a peptide in which Glu was replaced with Ile (TGWITWV<sub>COOH</sub>) interacted only with MAGI-3 PDZ2.<sup>[53]</sup> Recent three-dimensional structures and ho-

mology models have also shown that, at least in some cases, PDZ domains can make specific contacts with up to five C-terminal side chains.<sup>[52, 57]</sup> As shown for MAGI-3 PDZ2, the peptide main chain makes antiparallel  $\beta$ -sheet interactions with the PDZ domain main chain and the terminal carboxylate is inserted into a “carboxylate-binding loop” (Figure 7), and these interactions

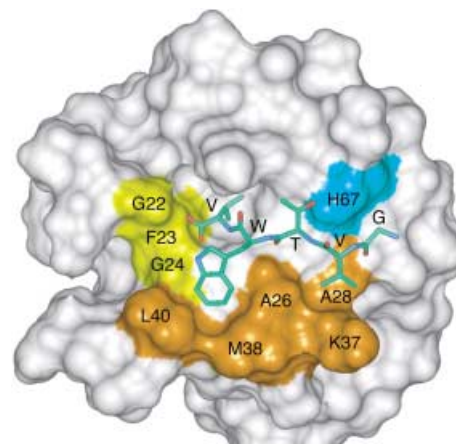


**Figure 7.** Molecular surface of a model of the MAGI-3 PDZ2 in complex with a peptide (GVTVW).<sup>[52]</sup> Protein residues conferring binding affinity and/or specificity are colored: yellow, the carboxylate-binding loop that interacts with the C-terminal residue Val5; orange, residues in  $\beta$  strands 2 and 3 that interact with the peptide side chains Trp4 and Val2; cyan, a conserved His residue that forms a hydrogen bond with Thr3.

are conserved amongst essentially all PDZ domains. The peptide resides in a groove on the PDZ domain surface and the peptide side chains can make contacts on either side; these contacts confer specificity to the interaction, since the types of ligand side chains accepted by a particular PDZ domain will depend on the nature of the protein surface. The fact that PDZ domains bind with high affinity and specificity to small linear peptides suggests that they may be valid small-molecule targets, and it is even possible that peptide ligands could be used as starting points for small-molecule design.

## 5. Summary and Outlook

In this review, we have highlighted the utility of phage display for investigating protein–protein interactions. Shotgun-scanning technology makes it possible to scan an extensive interface in detail in a matter of weeks, and peptide–phage libraries allow for the selection of unique ligands in a comparable time frame. These advances are accelerating the exploration of protein binding surfaces at a time when genomics and proteomics are revealing thousands of novel protein–protein interactions. We believe that phage display not only enables the rapid analysis of natural interactions, but also allows us to assess the potential of a binding surface as a small-molecule target.

While recognizing that we should not overgeneralize on the basis of experiences with a limited number of model systems, we feel that some trends have emerged. One observation is that, while protein mutagenesis studies have identified smaller

functional binding epitopes within large protein–protein interfaces, phage-displayed peptide libraries nonetheless yield binders with large contact surfaces in the majority of cases. When phage display yields only peptide ligands with extended binding surfaces, the validity of a protein as a small-molecule target is questionable. In contrast, proteins that bind to small, continuous epitopes may be very attractive small-molecule targets. While the results to date indicate that significant challenges still exist in developing small-molecule inhibitors of many protein–protein interactions, the good news is that phage display can be used to rapidly screen potential targets to identify those proteins with binding profiles that indicate the existence of potential binding sites for small molecules, and these insights should be useful in guiding medicinal chemistry efforts.

- [1] a) E. S. Lander et al., *Nature* **2001**, *409*, 860–921; b) J. C. Venter et al., *Science* **2001**, *291*, 1304–1351.
- [2] J. Pelletier, S. Sidhu, *Curr. Opin. Biotechnol.* **2001**, *12*, 340–347.
- [3] a) G. P. Smith, *Science* **1985**, 1315–1317; b) S. Bass, R. Greene, J. A. Wells, *Proteins: Struct. Funct. Genet.* **1990**, *8*, 309–314; c) J. K. Scott, G. P. Smith, *Science* **1990**, 386–390.
- [4] S. S. Sidhu, H. B. Lowman, B. C. Cunningham, J. A. Wells, *Methods Enzymol.* **2000**, *293*, 865–861.
- [5] a) G. P. Smith, V. A. Petrenko, *Chem. Rev.* **1997**, *97*, 391–410; b) S. S. Sidhu, *Curr. Opin. Biotechnol.* **2000**, *11*, 610–616.
- [6] C. J. Tsai, S. L. Lin, H. J. Wolfson, R. Nussinov, *Crit. Rev. Biochem. Mol. Biol.* **1996**, *31*, 127–152.
- [7] J. A. Wells, *Methods Enzymol.* **1991**, *202*, 390–411.
- [8] B. C. Cunningham, J. A. Wells, *Science* **1989**, *244*, 1081–1085.
- [9] T. Clackson, J. A. Wells, *Science* **1995**, *267*, 383–386.
- [10] B. C. Cunningham, J. A. Wells, *J. Mol. Biol.* **1993**, *234*, 554–563.
- [11] G. A. Weiss, C. K. Watanabe, A. Zhong, A. Goddard, S. S. Sidhu, *Proc. Natl. Acad. Sci. USA* **2000**, *97*, 8950–8954.
- [12] F. F. Vajdos, C. W. Adams, T. N. Breece, L. G. Presta, A. M. de Vos, S. S. Sidhu, *J. Mol. Biol.* **2002**, *320*, 415–428.
- [13] K. Deshayes, M. L. Schaffer, N. J. Skelton, G. R. Nakamura, S. Kadkhodayan, S. S. Sidhu, *Chem. Biol.* **2002**, *9*, 495–505.
- [14] A. G. Cochran, *Chem. Biol.* **2000**, *9*, R85–R94.
- [15] O. Livnah, E. A. Stura, D. L. Johnson, S. A. Middleton, L. S. Mulcahy, N. C. Wrighton, W. J. Dower, L. K. Jolliffe, I. A. Wilson, *Science* **1996**, *273*, 464–471.
- [16] O. Livnah, D. L. Johnson, E. A. Stura, F. X. Farrell, F. P. Barbone, Y. You, K. D. Liu, M. A. Goldsmith, W. He, C. D. Krause, S. Pestka, L. K. Jolliffe, I. A. Wilson, *Nat. Struct. Biol.* **1998**, *5*, 993–1003.
- [17] a) H. B. Lowman, Y. M. Chen, N. J. Skelton, D. L. Mortensen, E. E. Tomlinson, M. D. Sadick, I. C. Robinson, R. G. Clark, *Biochemistry* **1998**, *37*, 8870–8878; b) N. J. Skelton, S. Russell, F. de Sauvage, A. G. Cochran, *J. Mol. Biol.* **2002**, *316*, 1111–1125.
- [18] W. J. Fairbrother, H. W. Christinger, A. G. Cochran, G. Fuh, C. J. Keenan, C. Quan, S. K. Shriver, J. Y. K. Tom, J. A. Wells, B. C. Cunningham, *Biochemistry* **1998**, *37*, 17754–17764.
- [19] D. M. Eckert, V. N. Malashkevich, L. H. Hong, P. A. Carr, P. S. Kim, *Cell* **1999**, *99*, 103–115.
- [20] M. S. Dennis, C. Eigenbrot, N. J. Skelton, M. H. Ultsch, L. Santell, M. A. Dwyer, M. P. O'Connell, R. A. Lazarus, *Nature* **2000**, *404*, 465–470.
- [21] W. L. DeLano, M. H. Ultsch, A. M. de Vos, J. A. Wells, *Science* **2000**, *287*, 1279–1283.
- [22] T. Scherf, R. Kasher, M. Balass, M. Fridkin, S. Fuchs, E. Katchalski-Katzir, *Proc. Natl. Acad. Sci. USA* **2001**, *98*, 6629–6634.
- [23] G. R. Nakamura, M. A. Starovasnik, M. E. Reynolds, H. B. Lowman, *Biochemistry* **2001**, *40*, 9828–9835.
- [24] G. R. Nakamura, M. E. Reynolds, Y. M. Chen, M. A. Starovasnik, H. B. Lowman, *Proc. Natl. Acad. Sci. USA* **2002**, *99*, 1303–1308.
- [25] B. Pan, B. Li, S. J. Russell, J. Y. K. Tom, A. G. Cochran, W. J. Fairbrother, *J. Mol. Biol.* **2002**, *316*, 769–787.
- [26] a) J. Folkman, *Nature Med.* **1995**, *1*, 27–31; b) N. Ferrara, *Am. J. Physiol. Cell Physiol.* **2001**, *280*, C1358–C1366.
- [27] H. Gille, J. Kowalski, B. Li, J. LeCouter, B. Moffat, T. F. Zioncheck, N. Pelletier, N. Ferrara, *J. Biol. Chem.* **2001**, *276*, 3222–3230.
- [28] a) J. E. Park, H. H. Chen, J. Winer, K. A. Houck, N. Ferrara, *J. Biol. Chem.* **1994**, *269*, 25646–25654; b) S. Hiratsuka, O. Minowa, J. Kuno, T. Noda, M. Shibuya, *Proc. Natl. Acad. Sci. USA* **1998**, *95*, 9349–9354.
- [29] C. Wiesmann, G. Fuh, H. W. Christinger, C. Eigenbrot, J. A. Wells, A. M. de Vos, *Cell* **1997**, *91*, 695–704.
- [30] a) B. A. Keyt, L. T. Berleau, H. V. Nguyen, H. Chen, H. Heinsohn, R. Vandlen, N. Ferrara, *J. Biol. Chem.* **1996**, *271*, 7788–7795; b) G. Fuh, B. Li, C. Crowley, B. Cunningham, J. A. Wells, *J. Biol. Chem.* **1998**, *273*, 11197–11204; c) B. Li, G. Fuh, G. Meng, X. Xin, M. E. Gerritsen, B. Cunningham, A. M. de Vos, *J. Biol. Chem.* **2000**, *275*, 29823–29828.
- [31] Y. A. Muller, B. Li, H. W. Christinger, J. A. Wells, B. C. Cunningham, A. M. de Vos, *Proc. Natl. Acad. Sci. USA* **1997**, *94*, 7192–7197.
- [32] Y. A. Muller, Y. Chen, H. W. Christinger, B. Li, B. C. Cunningham, H. B. Lowman, A. M. de Vos, *Structure* **1998**, *6*, 1153–1167.
- [33] Y. Chen, C. Wiesmann, G. Fuh, B. Li, H. W. Christinger, P. McKay, A. M. de Vos, H. B. Lowman, *J. Mol. Biol.* **1999**, *293*, 865–881.
- [34] C. Wiesmann, H. W. Christinger, A. G. Cochran, B. C. Cunningham, W. J. Fairbrother, C. J. Keenan, G. Meng, A. M. de Vos, *Biochemistry* **1998**, *37*, 17765–17772.
- [35] B. K. Kay, A. V. Kurakin, R. Hyde-DeRuyscher, *Drug Discovery Today* **1998**, *8*, 370–378.
- [36] N. J. Skelton, Y. M. Chen, N. Dubree, C. Quan, D. Y. Jackson, A. Cochran, K. Zobel, K. Deshayes, M. Baca, M. T. Pisabarro, H. B. Lowman, *Biochemistry* **2001**, *40*, 8487–8498.
- [37] S. Jones, J. M. Thornton, *Prog. Biophys. Mol. Biol.* **1995**, *63*, 31–65.
- [38] D. R. Davies, E. A. Padlan, S. Sheriff, *Annu. Rev. Biochem.* **1990**, *59*, 439–473.
- [39] T. Pawson, *Nature* **1995**, *373*, 573–580.
- [40] R. Ren, B. J. Mayer, P. Cicchetti, D. Baltimore, *Science* **1993**, *259*, 1157–1161.
- [41] H. I. Chen, M. Sudol, *Proc. Natl. Acad. Sci. USA* **1995**, *92*, 7819–7823.
- [42] Z. Songyang, S. E. Shoelson, M. Chaudhuri, G. Gish, T. Pawson, W. G. Haser, F. King, T. Roberts, S. Ratnoffsky, R. J. Lechleider, *Cell* **1993**, *72*, 767–778.
- [43] W. M. Kavanaugh, L. T. Williams, *Science* **1994**, *266*, 1862–1865.
- [44] D. Cowburn, *Curr. Opin. Struct. Biol.* **1997**, *7*, 835–838.
- [45] a) A. B. Sparks, L. A. Quilliam, J. M. Thorn, C. J. Der, B. K. Kay, *J. Biol. Chem.* **1994**, *269*, 23853–23856; b) A. B. Sparks, J. E. Rider, N. G. Hoffman, D. M. Fowlkes, L. A. Quilliam, B. K. Kay, *Proc. Natl. Acad. Sci. USA* **1996**, *93*, 1540–1544; c) R. J. Rickles, M. C. Botfield, Z. Weng, J. A. Taylor, O. M. Green, J. S. Brugge, M. J. Zoller, *EMBO J.* **1994**, *13*, 5598–5604.
- [46] R. J. Rickles, M. C. Botfield, X.-M. Zhou, P. A. Henry, J. S. Brugge, M. J. Zoller, *Proc. Natl. Acad. Sci. USA* **1995**, *92*, 10909–10913.
- [47] a) B. Fazi, M. J. T. V. Cope, A. Douangamath, S. Ferracuti, K. Schirwitz, A. Zucconi, D. G. Drubin, M. Wilmanns, G. Cesareni, L. Castagnoli, *J. Biol. Chem.* **2002**, *277*, 5290–5298; b) A. M. Mongiovi, P. R. Romano, S. Panni, M. Mendoza, W. T. Wong, A. Musacchio, G. Cesareni, P. P. Di Fiore, *EMBO J.* **1999**, *18*, 5300–5309; c) G. Cestra, L. Castagnoli, L. Dente, O. Minenkova, A. Petrelli, N. Migone, U. Hoffmuller, J. Schneider-Mergener, G. Cesareni, *J. Biol. Chem.* **1999**, *274*, 32001–32007.
- [48] H. Linn, K. S. Ermekova, S. Rentschler, A. B. Sparks, B. K. Kay, M. Sudol, *Biol. Chem.* **1997**, *378*, 531–537.
- [49] A. H. Y. Tong, B. Drees, G. Nardelli, G. D. Bader, B. Brannetti, L. Castagnoli, M. Evangelista, S. Ferracuti, B. Nelson, S. Paoluzi, M. Quondam, A. Zucconi, C. W. V. Hogue, S. Fields, C. Boone, G. Cesareni, *Science* **2002**, *295*, 321–324.
- [50] a) H. Gram, R. Schmitz, J. F. Zuber, G. Baumann, *Eur. J. Biochem.* **1997**, *246*, 633–637; b) L. Dente, C. Vetriani, A. Zucconi, G. Pelicci, L. Lanfranccone, P. G. Pelicci, G. Cesareni, *J. Mol. Biol.* **1997**, *269*, 694–703.
- [51] a) S. Tomita, R. A. Nicoll, D. S. Bredt, *J. Cell. Biol.* **2001**, *153*, F19–F23; b) A. S. Fanning, J. M. Anderson, *Curr. Opin. Cell Biol.* **1999**, *11*, 432–439.
- [52] G. Fuh, M. T. Pisabarro, Y. Li, C. Quan, L. A. Lasky, S. S. Sidhu, *J. Biol. Chem.* **2000**, *275*, 21486–21491.
- [53] R. P. Laura, A. S. Witt, H. A. Held, R. Gerstner, K. Deshayes, M. F. T. Koehler, K. S. Kosik, S. S. Sidhu, L. A. Lasky, *J. Biol. Chem.* **2002**, *277*, 12906–12914.
- [54] J.-P. Borg, S. Marchetto, A. Le Bivic, V. Ollendorff, F. Jaulin-Bastard, H. Saito, E. Fournier, J. Adelaide, B. Margolis, D. Birnbaum, *Nat. Cell Biol.* **2000**, *2*, 407–414.



- [55] L. N. Klapper, M. H. Kirschbaum, M. Sela, Y. Yarden, *Adv. Cancer Res.* **2000**, 77, 25 – 79.
- [56] a) Q. Lu, N. K. Mukhopadhyay, J. D. Griffin, M. Paredes, M. Medina, K. S. Kosik, *J. Neurosci. Res.* **2002**, 67, 618 – 624; b) P. E. Fraser, G. Yu, L. Levesque, M. Nishimura, D. S. Yang, H. T. Mount, D. Westaway, P. H. St. George-Hyslop, *Biochem. Soc. Symp.* **2001**, 67, 89 – 100.
- [57] a) S. Karthikeyan, T. Leung, J. A. A. Ladas, *J. Biol. Chem.* **2001**, 276, 19683 – 19686; b) S. Karthikeyan, T. Leung, J. A. A. Ladas, *J. Biol. Chem.* **2002**, 277, 18973 – 18978.
- [58] A. M. de Vos, M. H. Ultsch, A. A. Kossiakoff, *Science* **1992**, 255, 306 – 312.
- [59] R. Koradi, M. Billeter, K. Wüthrich, *J. Mol. Graphics* **1996**, 14, 51 – 55.

---

Received: August 2, 2002 [A 469]